Available online at www.sciencedirect.com
ScienceDirect
Journal of the European Ceramic Society 30 (2010) 531–538
www.elsevier.com/locate/jeurceramsoc

Effect of thermal annealing on electrical degradation characteristics of Sb–Bi–Mn–Co-added ZnO varistors

Masayuki Takada, Shinzo Yoshikado *

Faculty of Science and Engineering, Doshisha University, 1-3 Tatara-miyakodani, Kyotanabe 610-0321, Japan

Available online 16 July 2009

Abstract

The effects of thermally annealing Bi–Mn–Co–Sb_2O_3-added ZnO varistors on their electrical degradation were investigated. For the samples added with 0.01 mol% Sb_2O_3 and without Sb_2O_3, no marked difference in the nonlinearity index α of the voltage–current (V–I) characteristics was observed upon electrical degradation for the annealed and nonannealed samples. Upon increasing the amount of Sb_2O_3 added, the values of α increased after electrical degradation for the annealed samples. Moreover, the value of α after electrical degradation was proportional to the width of gauss function (width) of the X-ray diffraction peak for $Zn_{2.33}Sb_{0.67}O_4$-type spinel particles under various annealing conditions. The added Sb_2O_3 did not dissolve in the ZnO grains but became segregated at grain boundaries. Therefore, it is speculated that the increase in the width of the spinel particles is due to the increase in the numbers of fine spinel particles at grain boundaries and triple points. Furthermore, it is suggested that the improvement of the electrical degradation is due to the decrease in the mobility of oxide ions or Zn^{2+} ions owing to their being blocked by uniformly dispersed fine spinel particles at grain boundaries.

Keywords: ZnO; Varistor; Electrical degradation; Grain boundaries

1. Introduction

The nonlinear voltage–current (V–I) characteristics of a ZnO varistor are explained using a basic model of symmetrical double Schottky barriers formed at grain boundaries.[1] The deterioration of V–I characteristics progresses with voltage application, and the nonlinearity is eliminated.[1] This deterioration can be explained as follows: the disappearance of nonlinearity is caused by the redistribution of electrons and holes near grain boundaries owing to the movement of oxide ions and interstitial Zn^{2+} ions across grain boundaries and around the neighborhood of grain boundaries as a result of the electric field created by the applied voltage.[2–6] Moreover, an interstitial Zn^{2+} ion between lattice ions has mobility in a grain of ZnO and generation energy comparable to that of an oxide ion; both of these ions may contribute to electrical degradation.[7]

Varistors with good characteristics can be obtained by adding Sb_2O_3 to ZnO varistors. However, Sb_2O_3-free varistors with good characteristics are now in demand owing to the toxicity of Sb_2O_3. At the present stage, it is necessary to clarify the effect of Sb_2O_3 addition on the electrical degradation characteristics of ZnO varistors. At present, the improvement of the electrical degradation of ZnO varistors can be achieved by adding several impurities, such as Si, Sb or by thermal annealing or humidity.[4,8–15] Upon the addition of Sb_2O_3 to a Bi–Mn–Co-added ZnO varistor, changes in the grain boundary structure such as the formation of a twin crystal of ZnO, the formation of $Zn_{2.33}Sb_{0.67}O_4$-type spinel structures (hereafter, spinel particles), and changes in the orientation of ZnO grains and the crystal structure of Bi_2O_3 occur.[9,10,16–18] It has been reported that the changes in the grain boundary structure affect the electrical degradation characteristics of varistors as a result of the change in the mobility of oxide ions or Zn^{2+} ions at grain boundaries and in ZnO grains near the grain boundary.[9,10] In previous studies, the effect of annealing on electrical degradation characteristics of ZnO varistors has been reported. The decrease in the number of interstitial Zn^{2+} ions or the phase transition of Bi_2O_3 upon annealing causes the improvement of the electrical degradation.[4,13] However, the effect of Sb addition on the improvement of the electrical degradation of ZnO varistors upon annealing is not clarified. In this study, samples of thermally annealed Sb_2O_3-added ZnO varistors were prepared to investigate the effect of annealing on the tolerance characteristics of electrical degradation, and the relationship between

* Corresponding author. Tel.: +81 774 65 6328.
E-mail address: syoshika@mail.doshisha.ac.jp (S. Yoshikado).

0955-2219/$ – see front matter © 2009 Elsevier Ltd. All rights reserved.
doi:10.1016/j.jeurceramsoc.2009.06.006

the change in the grain boundary structure, such as the formation of spinel particles or the phase transition of the Bi_2O_3 phase, and the electrical degradation characteristics were investigated. The structure of grain boundaries and ZnO grains, the element-mapping profile, and the crystal structure were studied by field-emission scanning electron microscopy (FE-SEM), energy dispersion X-ray spectroscopy (EDS), backscattered-electron (BSE) analysis, and powder X-ray diffraction (XRD) analysis. Electrical characteristics were determined on the basis of the *V–I* plot.

2. Experiments

ZnO varistors were fabricated using ZnO (Meidensha Corporation, purity: 99.999%), Bi_2O_3 (purity: 99.9%), MnO_2 (purity: 99.99%), Co_3O_4 (purity: 99.99%) and $SbCl_3$ (purity: 99.8%; hereafter, Sb_2O_3) powders. The composition of each component was determined such that the total mol% was 100 mol%, i.e., ZnO–Bi_2O_3 (0.5 mol%)–MnO_2 (0.5 mol%)–Co_3O_4 (0.2 mol%)–Sb_2O_3 (0∼0.5 mol%). Predetermined amounts of ZnO powder and added impurities were wet-mixed for 24 h in a nylon ball mill using ethanol to prevent their mixing with Al and Si, which markedly affects the characteristics of ZnO varistors. After drying the mixed powder, the samples were presintered at 600 °C for 5 h in air, and then ground in an agate mortar for a short time to prevent mixing of Si as much as possible. The ground powder was pressurized (320 MPa) and reshaped into 20-mm-diameter disks in vacuum. After sintering at 1150 °C for 3 h in air, samples were thermally treated by one of the following five types of temperature history. Type 1: rapidly cooled to room temperature by removing from the electric furnace. Type 2: naturally cooled to room temperature in the electric furnace. Type 3: cooled to room temperature at a rate of 240 °C/h. Type 4: naturally cooled to room temperature in the electric furnace and then annealed at 700 °C for 5 h, followed by natural cooling to room temperature. Type 5: cooled at a rate of 240 °C/h to 700 °C and then annealed at 700 °C for 5 h, followed by natural cooling to room temperature. Samples were also thermally treated according to the following temperature histories after sintering: cooling at a rate of 240 °C/h to 500, 700, or 900 °C, followed by annealing for 1–10 h at the temperature and natural cooling to room temperature. After polishing a disk to 0.5 mm thickness and washing it, 2.38-mm-diameter aluminum electrodes were formed on both faces of each sample by vacuum evaporation. *V–I* characteristics were obtained in the current range of 10^{-8} to 10^{-4} A by a dc constant-current method (KEITHLEY, 2410-type source meter) to prevent the samples from undergoing electrical degradation due to voltage application. In this study, the nonlinear index α was obtained using

$$I = I_N \left(\frac{V}{V_{1\,\mathrm{mA}}} \right)^{\alpha} \tag{1}$$

where I_N is a constant and $V_{1\,\mathrm{mA}}$ is the voltage when the current density is 1 mA/cm^2; this voltage is a measure of the breakdown voltage of a varistor and is hereafter called varistor voltage. The same samples were used to obtain the *V–I* characteristics before and after electrical degradation. The electrical degradation was induced by applying a current density of 100 mA/cm^2 in air and the total duration of current conduction was 30 min. During electrical degradation, the samples were cooled in air and the temperature was maintained at approximately +30 °C or lower by air cooling with a blower. Values of α before and after electrical degradation were estimated from the inclination of *V–I* curves in the breakdown region from 0.1 to 1 mA/cm^2. A Multiflex instrument (Rigaku Corporation) was used for XRD analysis. The width of gauss function (width) of the X-ray diffraction peak for spinel particles was calculated using gauss function of Eq. (1) given by

$$I_{\mathrm{XRD}}(2\theta) = I_0 \exp\left[-\left(\frac{2\theta - 2\theta_0}{\mathrm{width}} \right)^2 \right] \tag{2}$$

Here, 2θ is the angle of the diffraction peak, I_{XRD} (2θ) is the diffraction peak intensity at 2θ, I_0 is a constant, $2\theta_0$ is the angle for maximum intensity of the diffraction peak and width is the width of gauss function. Measurements were carried out by placing the polished (pressurized) surface of each sample parallel to the sample table. A JSM7500FA (SEM; JEOL) was used for FE-SEM, BSE and EDS analysis.

3. Results and discussion

3.1. Dependence of α on annealing temperature history

For the sample added with 0.12 mol% Sb_2O_3, with which the degree of improvement of the electrical degradation characteristics was the lowest, the degree of improvement of the degradation characteristic was investigated for samples annealed with the five types of temperature history described above. Fig. 1 shows the values of α before and after electrical degradation for various annealing temperature histories. Before electrical degradation, the α value of the sample with Type 1 annealing was approximately 40, which is slightly smaller than those of samples annealed with other types of history (approximately 45–50). After electrical degradation, the α values of the samples annealed with Types 1 and 2 histories were approximately 2 and 5, respectively, and those of the samples annealed with other types of history were approximately 15. It was found that the electrical degradation characteristics could be improved by particular annealing temperature histories. The α values of the

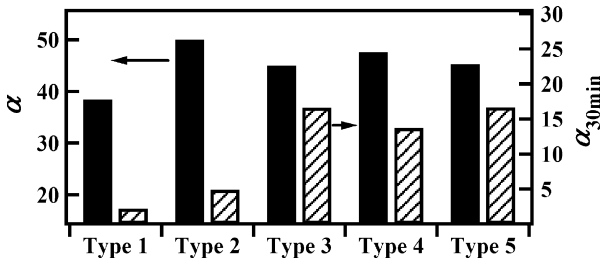

Fig. 1. Values of α before and after electrical degradation for each type of annealing history.

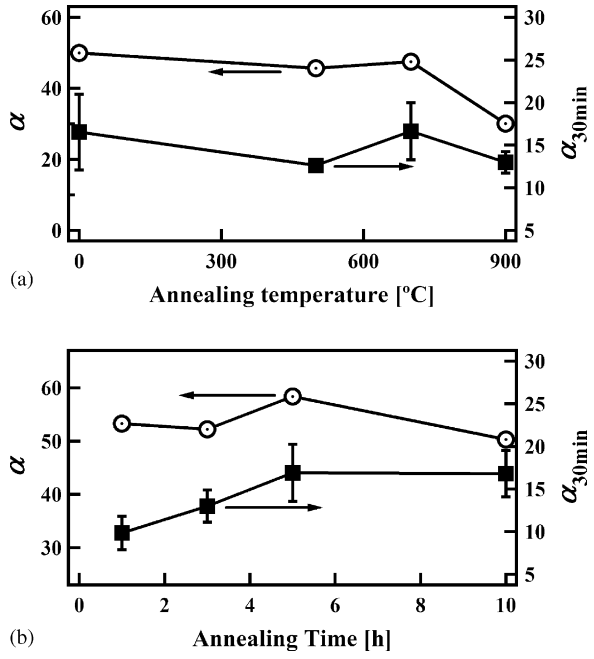

Fig. 2. Values of α before and after electrical degradation for samples with 0.12 mol% Sb_2O_3 under (a) various annealing temperatures and (b) various annealing times.

samples annealed with Types 1–3 histories increase with slower the cooling rates.

3.2. Dependence of α on annealing temperature and time

Fig. 2(a) shows the values of α before and after electrical degradation of samples added with 0.12 mol% Sb_2O_3 and cooled at a rate of 240 °C/h to 500, 700, or 900 °C, followed by annealing for 5 h and then natural cooling to room temperature. Fig. 2(b) shows the values of α before and after electrical degradation of samples added with 0.12 mol% Sb_2O_3 and cooled at a rate of 240 °C/h to 700 °C, followed by annealing for 1–10 h and then natural cooling to room temperature. Before electrical degradation, values of α were approximately 50 for samples annealed at 500 and 700 °C, and with Type 5 annealing and approximately 30 for the sample annealed at 900 °C. After electrical degradation, values of α for those samples were approximately 15. It has also been reported that interstitial Zn^{2+} ions were removed sufficiently at annealing temperatures from 600 to 800 °C.[4] Therefore, henceforth, annealing temperature was fixed at 700 °C. As shown Fig. 2(b), before electrical degradation, the value of α did not depend on annealing time, but after electrical degradation, α increased with increasing annealing time up to approximately 5 h and then became almost constant over 5 h.

3.3. Dependence of effects of annealing on amount of Sb_2O_3 addition

Fig. 3(a) and (b) shows the values of α after electrical degradation for the samples with various amounts of Sb_2O_3 annealed at 700 °C for 5 h with Types 4 and 5 histories. Without annealing,

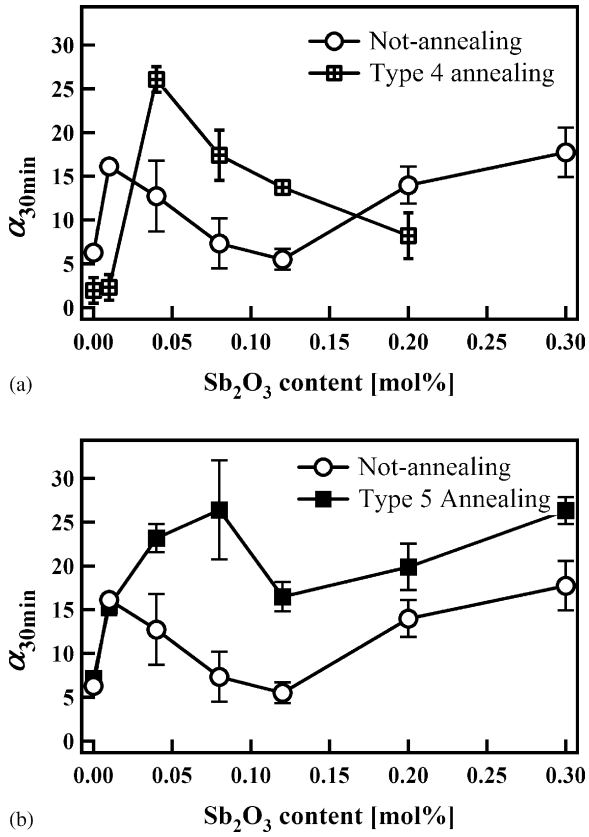

Fig. 3. Values of α after electrical degradation for nonannealed and annealed Sb_2O_3-added samples: (a) Type 4 annealing and (b) Type 5 annealing.

α of the sample with 0.01 mol% Sb_2O_3 increased. α decreased with increasing amount of Sb_2O_3 up to 0.12 mol%, as shown in Fig. 3(a). However, α increased again for the samples with more than 0.12 mol% Sb_2O_3 addition. After Type 4 annealing, α after electrical degradation for the samples with 0.01 mol% Sb_2O_3 and without Sb_2O_3 were approximately 2, and that for the sample with 0.04 mol% Sb_2O_3 increased rapidly and had the local maximum value of 25. Then, α decreased as the amount of Sb_2O_3 increased to more than 0.04 mol%. With Type 5 annealing, α increased for the samples with more than 0.01 mol% Sb_2O_3, although the samples with up to 0.01 mol% Sb_2O_3 showed no difference in the value of α. This result indicated that the tolerance characteristics of varistors to electrical degradation are unchanged or deteriorated upon annealing for samples with up to 0.01 mol% Sb_2O_3. In contrast, the tolerance characteristics of varistors to electrical degradation were improved markedly by the addition of more than 0.01 mol% Sb_2O_3, except for the sample with 0.2 mol% Sb_2O_3 and Type 4 annealing. Thus, it was found that the tolerance characteristics of varistors to electrical degradation after annealing greatly depend on the amount of Sb_2O_3 added. The model of electrical degradation has been proposed by Eda et al.[2] and Gupta and Carlson.[4] This model is explained as follows: interstitial Zn^{2+} or oxide ions move to the grain boundary and inside grain when the electric field is applied. Consequently, Schottky barriers are distorted, such as the decrease of Schottky barrier height.

It is speculated that lattice defects in the crystal and the crystal structure in thermal equilibrium at 1150 °C are partly retained for the nonannealed samples with Types 1 and 2 histories, while the samples annealed at 700 °C partly have a thermal equilibrium at 700 °C. Therefore, three factors behind changes in thermal equilibrium are considered as follows: (A) the number of Zn^{2+} ions between among a lattice of ZnO grains, (B) crystal structure of Bi_2O_3, and (C) formation of compounds such as spinel particles. These changes deeply correlate with the variation of the tolerance characteristics of varistors upon electrical degradation caused by thermal annealing. In the next section, we discuss these factors.

3.4. Relationship between change in orientation of ZnO grains caused by annealing and electrical degradation characteristics

The composition of elements within spinel particles measured by EDS analysis showed no difference upon annealing. A similar tendency was confirmed for various annealing times. Moreover, only Mn and Co were observed within ZnO grains, which were obtained under the limit of EDS detection. The composition of ZnO grains in annealed samples showed no difference from those of the nonannealed samples. In contrast, it has been reported that the crystal structure of Bi_2O_3 at grain

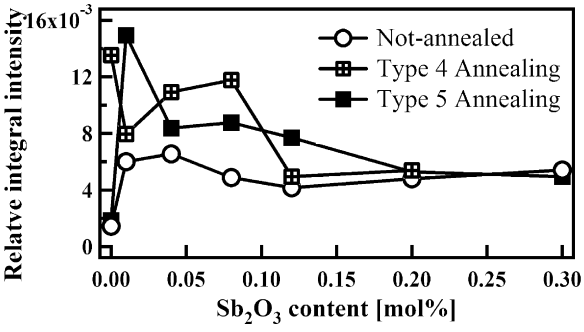

Fig. 4. Relative integral intensity of XRD diffraction peak for (0 0 4) plane of ZnO grains for nonannealed and annealed samples with various Sb_2O_3 contents.

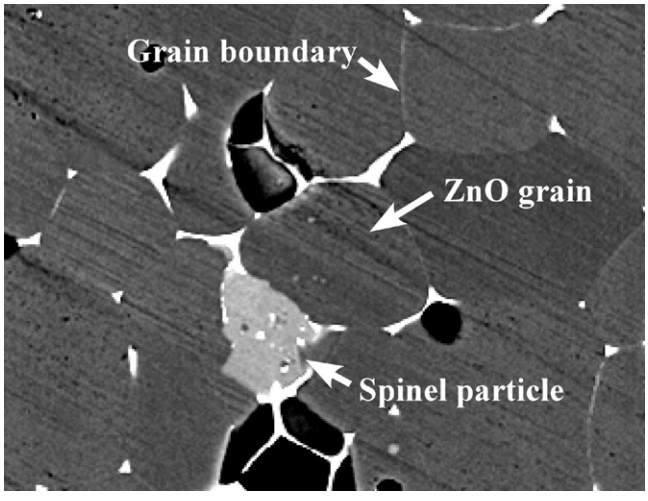

Fig. 5. BSE image of samples with 0.12 mol% Sb_2O_3.

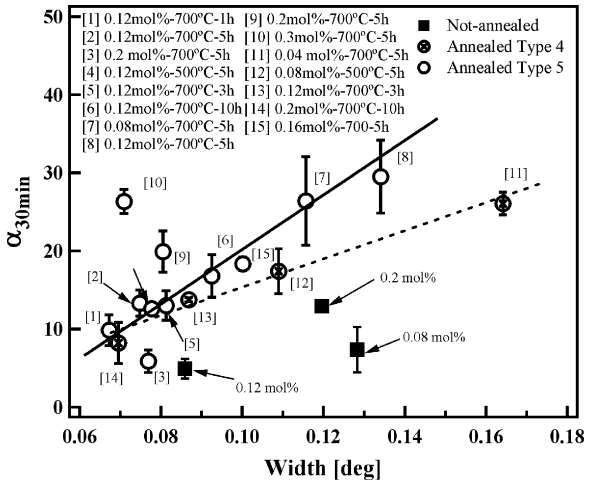

Fig. 6. Relationship between values of α after electrical degradation and the width of diffraction peaks for spinel particles for various annealing conditions.

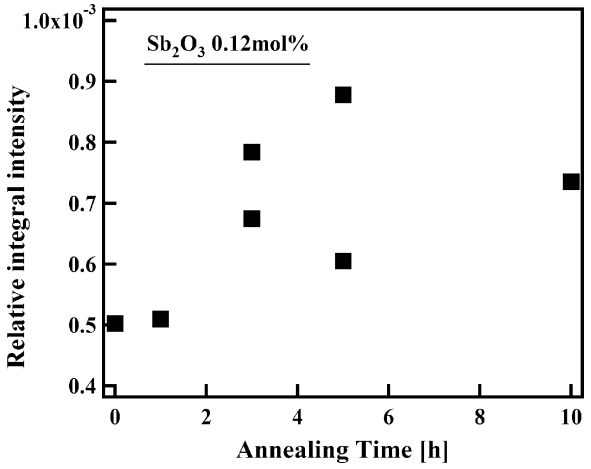

Fig. 7. Relative integral intensity of spinel particles for samples with 0.12 mol% Sb_2O_3 and various annealing times.

boundaries changes to the α, γ, or δ-type structure owning to the composition of impurities added or the sintering and annealing conditions.[8–10,16,19–21] However, in this study, it was found that the degree of electrical degradation is related to other factors in

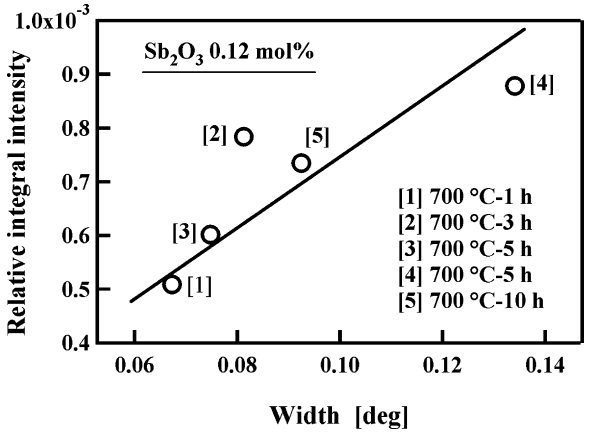

Fig. 8. Relationship between relative integral intensity and width of the XRD peaks for spinel particles.

addition to the crystal structure of Bi_2O_3. Furthermore, it has been reported that the electrical degradation characteristics of samples with 0.1 mol% Sb_2O_3 or less is correlated to the orientation of ZnO grains; this is because the mobility of oxide ions or Zn^{2+} ions depends on the orientation of ZnO grains.[9,10] Fig. 4 shows the relative integral intensity of the diffraction peak for the (0 0 4) plane of ZnO grains of Sb_2O_3-added samples before and after annealing. The intensity for the sample without Sb_2O_3 rapidly increased after Type 4 annealing, those of the annealed samples decreased with increasing amount of Sb_2O_3 up to approximately 0.12 mol% or more, and those of the nonannealed samples were almost constant. The peak intensity of the (0 0 4) plane of the sample with 0.01 mol% Sb_2O_3 with Type 5 annealing increased more rapidly than that of the nonannealed sample and then decreased with increasing amount of Sb_2O_3. For the samples with 0.2 mol% Sb_2O_3 or more, the peak inten-

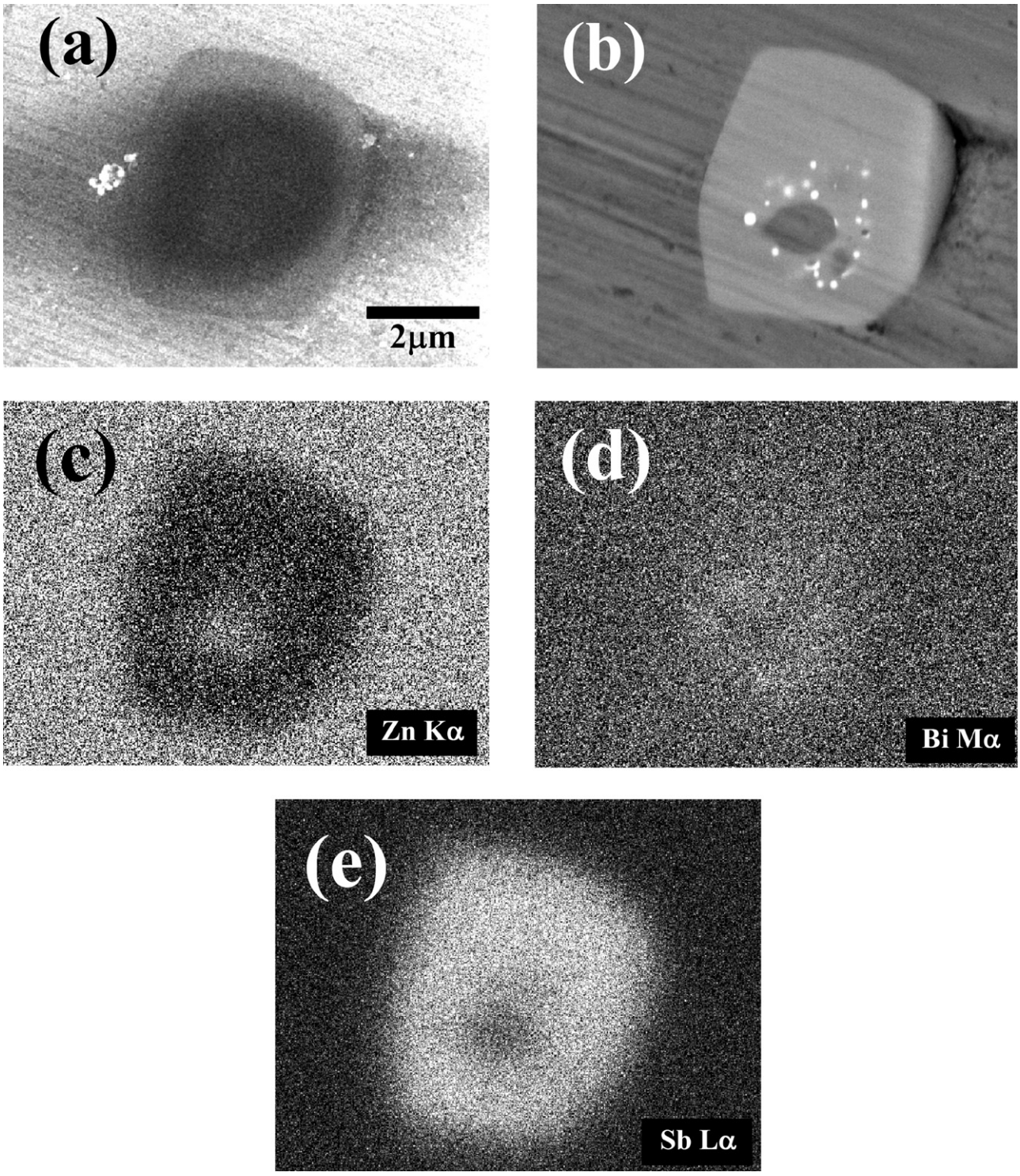

Fig. 9. (a) SEM image, (b) BSE image, and elemental mappings of spinel particles for nonannealed samples with 0.12 mol% Sb_2O_3, (c) Zn, (d) Sb, and (e) Sb.

sity for annealed samples agreed with that of the nonannealed sample. Moreover, the peak intensity of the (0 0 4) plane of samples with 0.12 mol% Sb_2O_3 and Type 5 annealing as a function of annealing time and temperature was almost constant under various annealing conditions. It was found that the peak intensity of the (0 0 4) plane of the samples with 0.12 mol% Sb_2O_3 or less increased upon annealing. For the samples with Sb_2O_3 and annealed at 700 °C, before electrical degradation, the values of α after thermal annealing were approximately 40 to 60 for all amounts of added Sb_2O_3 and the values of α did not change upon annealing. For the samples with 0.01 mol% Sb_2O_3 and without Sb_2O_3, there was no marked difference in values of α after electrical degradation upon annealing. Therefore, it was found, for the samples with 0.12 mol% Sb_2O_3, the improvement of electrical degradation upon annealing is not affected by the peak intensity of the (0 0 4) plane of ZnO.

3.5. Relationship between formation of spinel particles and electrical degradation characteristics

As shown in Fig. 5, spinel particles are formed at grain boundaries and triple points upon a Sb_2O_3 addition. In a previous study, at the amount of added Sb_2O_3, with which spinel particles were formed, the value of α after electrical degradation increased from its minimum value.[10] It is suggested that there is a strong correlation between the formation of spinel particles at both grain boundaries and the triple points and the electrical degradation.[10] Fig. 6 shows the relationship between the value of α after electrical degradation upon Types 4 and 5 annealing and the width of gauss function (width) of the X-ray diffraction peak at 29.4° for the spinel particle. Moreover, the width changed upon annealing for the samples with 0.12 mol% Sb_2O_3 or less. For the same samples, the value of α after electrical degradation was proportional to the width of the diffraction peak for spinel particles, with annealing under various conditions. This result shows that there appears to be a correlation between the electrical degradation characteristics and the width for spinel particles at grain boundaries. On the other hand, no such correlation was apparent for samples with 0.2 mol% Sb_2O_3 or more. It is considered that there are two factors behind the broadening of the width of the diffraction peak for spinel particles upon annealing: (A) deterioration of the crystallinity of spinel particles and (B) formation of fine spinel particles upon annealing. As shown in Fig. 6, the width of the diffraction peak for spinel particles after annealing decrease. Therefore, it is unlikely that the increase in the width of annealed samples is due to the deterioration of crystallinity of spinel particles.

Next, let us discuss factor (B). Fig. 7 shows the relative integral intensity of diffraction peaks for the spinel particle of the sample with 0.12 mol% Sb_2O_3 and Type 5 annealing as a function of annealing time. The intensity increased with annealing for 3 h or more. It is considered that there are two factors explaining this result: first, the increase in the volume of the spinel particles that already existed; second, the formation of new spinel particles. Fig. 8 shows the relationship between the intensity and width of the diffraction peak for spinel particles. The intensity is proportional to the width. Therefore, the increase in the width is correlated to the increase in the intensity of the diffraction peak of the spinel particle. Spinel particles in samples with 0.12 mol% Sb_2O_3 and Type 4 annealing were observed by SEM and BSE analysis to estimate the change in their shape or volume after annealing. Here, the same spinel particles were observed before and after annealing. The shapes of 10 spinel particles on the pressurized surface or the side surface of a disk sample were observed. Fig. 9 shows the (a) SEM image, (b) BSE image, and (c)–(e) elemental mappings of spinel particles. In Fig. 9(b), the light-gray part in the BSE image is spinel particles containing mainly Sb. The composition mapping using the BSE image of spinel particles at grain boundaries and triple points was much sharper than that using EDS. In the BSE image, the inside of a spinel particle was spotted with Bi-rich particles and Zn-rich particles of approximately 80 nm and 0.5 μm diameters, respectively. For spinel particles on the pressurized surface, the

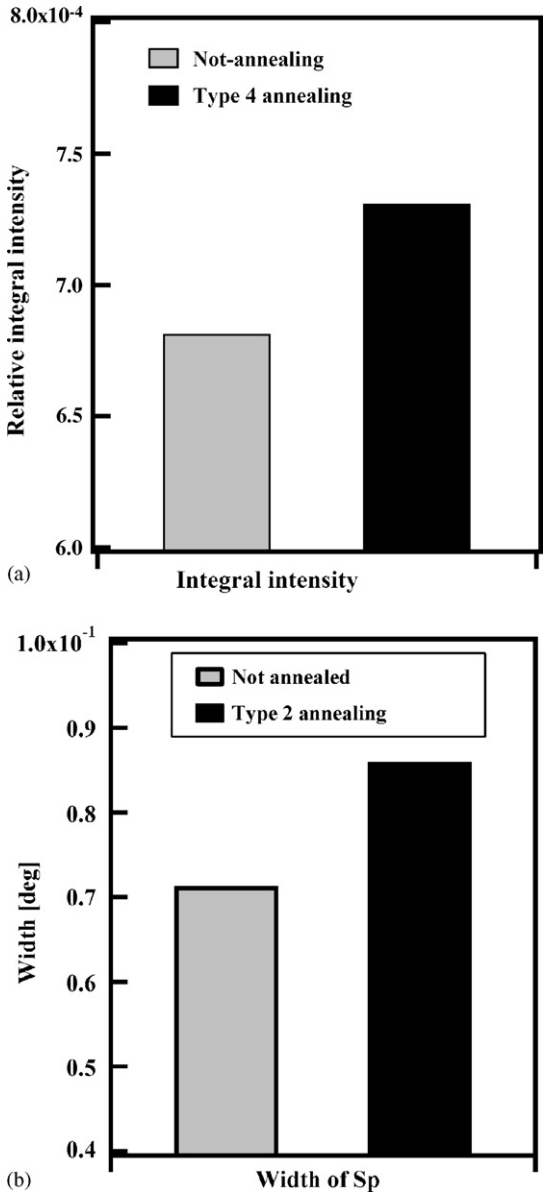

Fig. 10. (a) Relative integral intensity and (b) width of spinel particles for nonannealed and annealed samples.

cross-sectional areas of a spinel particle before and after annealing were almost the same. A similar tendency was confirmed for the spinel particle on the side surface. Therefore, it was found that the volume of spinel particles that already existed in the sample, did not increase upon annealing at 700 °C. Fig. 10 shows the relative integral intensity and the width of the diffraction peak for spinel particles before and after annealing. As a result, both the intensity and the width for a sample with 0.12 mol% Sb_2O_3 increased, and the intensity increased by approximately 1.1 times upon annealing. Thus, it was found that the increase in the intensity of the diffraction peak for spinel particles is due to the increase not in the volume of existing spinel particles but in the number of fine spinel particles newly formed at grain boundaries or triple points, and that the width of the diffraction peak for spinel particles is strongly correlated to the electrical degradation characteristics of ZnO varistors. In addition, the conductivity of the ion which passes through the spinel particle is speculated to be low compared with that of Bi_2O_3. This is because Bi_2O_3 segregated at grain boundary is an oxygen ion conductor with high conductivity.[18,22] Therefore, it is speculated that the ionic conductivity decreases owing to the fine spinel particle formed at grain boundary. Furthermore, it is suggested that the improvement in the electrical degradation is due to the decrease in the mobility of oxide ions or Zn^{2+} ions owning to be their being blocked by fine spinel particles at grain boundaries.

4. Conclusions

The relationship between the change in the crystal structure of spinel particles at grain boundaries and the electrical degradation was investigated in detail to discuss the effects of the thermal annealing of Bi–Mn–Co–Sb_2O_3-added ZnO varistors on electrical degradation. The following results were obtained:

(1) The electrical degradation characteristics were improved by annealing with slow cooling or annealing at 700 °C for 5 h. It was found that the tolerance characteristics of varistors to electrical degradation after annealing strongly depend on the amount of added Sb_2O_3.
(2) For the samples with Sb_2O_3, the improvement of electrical degradation upon annealing is not affected by the intensity of the diffraction peak of the (0 0 4) plane for ZnO.
(3) For samples with 0.12 mol% Sb_2O_3 or less, the nonlinearity index α of *V–I* characteristics after electrical degradation increased proportionally to the width of the diffraction peak for spinel particles in samples annealed under various conditions. It was found that the width strongly depends on both the annealing condition and the amount of added Sb_2O_3, and that the increase in the width is due to the formation of new fine spinel particles at grain boundaries or triple points induced by annealing. It is suggested that the improvement of electrical degradation is due to the decrease in the mobility of oxide ions or Zn^{2+} ions owing to their being blocked by uniformly dispersed fine spinel particles at grain boundaries.
(4) The composition image of spinel particles at grain boundaries and triple points using BSE were much sharper than that using EDS. In the BSE image, the inside of the spinel particle was spotted with Bi-rich particles and Zn-rich particles of approximately 80 nm and 0.5 μm diameters, respectively.

Acknowledgements

This study was supported by the RCAST of Doshisha University and the Joint Research Project in the Kyoto Prefectural Area. We thank Professor A. Ametani of Doshisha University and Mr. Masao Hayashi of MSA Corporation for providing us with this research opportunity.

References

1. Eda, K., Conduction mechanism of non-ohmic zinc oxide ceramics. *J. Appl. Phys.*, 1978, **49**, 2964–2972.
2. Eda, K., Iga, A. and Matuoka, M., Degradation mechanism of non-ohmic zinc oxide ceramics. *J. Appl. Phys.*, 1980, **51**(10), 2678–2684.
3. Mahan, G. D., Intrinsic defects in ZnO varistors. *J. Appl. Phys.*, 1983, **54**, 3825–3832.
4. Gupta, T. K. and Carlson, W. G., A grain boundary defect model for instability/stability of a ZnO varistor. *J. Mater. Sci.*, 1985, **20**, 3487–3500.
5. Ramanachalam, M. S., Rohatgi, A., Schaffer, J. P. and Gupta, T. K., Characterization of ZnO varistor degradation using lifetime positron nihilation spectroscopy. *J. Appl. Phys.*, 1991, **69**, 8380–8386.
6. Chiang, Y. M., Kingery, W. D. and Levinson, L. M., Compositional changes adjacent to grain boundaries during electrical degradation of a ZnO varistor. *J. Appl. Phys.*, 1982, **53**, 1765–1768.
7. Tomlins, G. W., Routbort, J. L. and Mason, T. O., Zinc self-diffusion, electrical properties, and defect structure of undoped single crystal zinc oxide. *J. Appl. Phys.*, 2000, **87**, 117–123.
8. Satoi, Y., Hirai, H., Yoshino, H. and Yoshikado, S., The effect of Si addition on electrical degradation of ZnO varistors. *Key Eng. Mater.*, 2004, **269**, 83–86.
9. Takada, M. and Yoshikado, S., Relation between grain boundary and electrical degradation of ZnO varistors. *Key Eng. Mater.*, 2006, **320**, 117–120.
10. Takada, M. and Yoshikado, S., Effect of SnO_2 addition on electrical degradation of ZnO varistors. *Proc. 10th. Eur. Ceram. Soc.*, 2007, 507–514.
11. Fan, J. and Freer, R., The electrical properties and d.c. degradation characteristics of silver doped ZnO varistors. *J. Mater. Sci.*, 1993, **28**, 1391–1395.
12. So, S. J. and Park, C. B., Improvement in the electrical stability of semiconducting ZnO ceramic varistors with SiO_2 additive. *J. Korean Phys. Sci.*, 2002, **40**, 925–929.
13. Shao, H. Q., Gao, X. H. and Cao, Z. C., Effect of annealing on phase structure and degradation of a zinc oxide varistor with Si-additive. *J. Eur. Ceram. Sci.*, 1997, **17**, 55–59.
14. Ivanchenko, A. V., Tonkoshkur, A. S. and Makarov, V. O., Desorption thermal degradation model of zinc oxide ceramics. *J. Eur. Ceram. Sci.*, 2003, **24**(15–16), 3709–3712.
15. Wang, M., Hu, K., Zhao, B. and Zhang, N., Degradation phenomena due to humidity in low voltage ZnO varistors. *Ceram. Int.*, 2007, **33**, 151–154.
16. Inada, M., Crystal phases of nonohmic zinc oxide ceramics. *Jpn. J. Appl. Phys.*, 1978, **17**, 1–10.
17. Takemura, T., Kobayashi, M., Takada, Y. and Sato, K., Effects of antimony oxide on the characteristics of ZnO varistors. *J. Am. Ceram. Soc.*, 1987, **70**, 237–241.
18. Richard, J. D. Tilley, *Defects in Solids*. John Wiley & Sons, Inc., New York, 2008, pp. 124–126.
19. Iga, A., Matuoka, M. and Masuyama, T., Effect of phase transition of intergranular Bi_2O_3 layer in nonohmic ZnO ceramics. *Jpn. J. Appl. Phys.*, 1976, **15**, 1161–1162.

20. Takemura, T., Kobayashi, M., Takada and Sato, K., High-temperature X-ray diffraction measurements of ZnO varistor. *Jpn. J. Appl. Phys.*, 1986, **25**, 295–296.
21. Kobayashi, K., Wada, O., Kobayashi, M. and Takada, Y., Continuous existence of bismuth at grain boundaries of zinc oxide varistor without intergranular phase. *J. Am. Ceram. Soc.*, 1998, **81**, 2071–2076.
22. Takahashi, T., Iwahara, H. and Arao, T., High oxide ion conduction in sintered oxides of the system Bi_2O_3-Y_2O_3. *J. Appl. Electrochem.*, 1975, **5**, 187–195.